

Determination of Generalized Parton Distributions (GPDs)

Muhammad Goharipour

Institute for Research in Fundamental Sciences (IPM)
In collaboration with H. Hashamipour, K. Azizi, and S. Goloskv

Weekly Seminar

March 1, 2023

Introduction

Generalized Parton Distributions (GPDs)
GPDs VS Observables
Determination of GPDs
Backup

Probing the Structure of the Proton
Elastic Scattering from a Finite Size Proton
Electromagnetic Form Factors (FFs)
Deep Inelastic Scattering (DIS)
Elastic VS Inelastic
Parton Distribution Functions (PDFs)

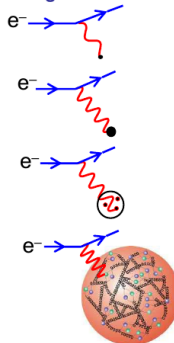
Introduction

Probing the Structure of the Proton

Probing the Structure of the Proton

★ In $e p \rightarrow e' p$ scattering the nature of the interaction of the virtual photon with the proton depends strongly on wavelength

- At **very low** electron energies $\lambda \gg r_p$:
the scattering is equivalent to that from a “point-like” spin-less object
- At **low** electron energies $\lambda \sim r_p$:
the scattering is equivalent to that from a extended charged object
- At **high** electron energies $\lambda < r_p$:
the wavelength is sufficiently short to resolve sub-structure. Scattering from constituent quarks
- At **very high** electron energies $\lambda \ll r_p$:
the proton appears to be a sea of quarks and gluons.



Elastic Scattering from a Finite Size Proton

★ In general the finite size of the proton can be accounted for by introducing **two structure functions**. One related to the **charge distribution** in the proton, $G_E(q^2)$ and the other related to the distribution of the **magnetic moment** of the proton, $G_M(q^2)$

$$\frac{d\sigma}{d\Omega} = \frac{\alpha^2}{4E_1^2 \sin^4 \theta/2} \frac{E_3}{E_1} \left(\frac{G_E^2 + \tau G_M^2}{(1 + \tau)} \cos^2 \frac{\theta}{2} + 2\tau G_M^2 \sin^2 \frac{\theta}{2} \right)$$

with the Lorentz Invariant quantity:

$$\tau = -\frac{q^2}{4M^2} > 0$$

Electromagnetic Form Factors (FFs)

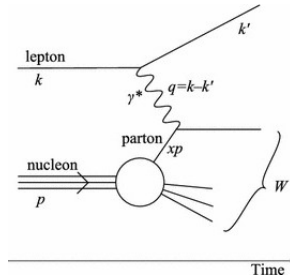
G_E and G_M are the **Sachs form factors (FFs)**. We can interpret the FFs in terms of the Fourier transforms of the charge and magnetic moment distributions.

$$G_E(q^2) = \int e^{i\vec{q}\cdot\vec{r}} \rho(\vec{r}) d^3\vec{r}$$

$$G_M(q^2) = \int e^{i\vec{q}\cdot\vec{r}} \mu(\vec{r}) d^3\vec{r}$$

Note: $t = (p_4 - p_2)^2 = (p_3 - p_1)^2 = q^2$

Deep Inelastic Scattering (DIS)



$$W^2 = (p + q)^2 = M_p^2 + 2p \cdot q + q^2$$

$$W^2 \gg M_p^2 \Rightarrow \text{Inelastic scattering}$$

$$Q^2 \gg M_p^2 \Rightarrow \text{Deep}$$

$$Q^2 = -q^2$$

$$x = \frac{Q^2}{2p \cdot q}$$

Elastic VS Inelastic

Elastic Scattering: Only one independent variable. We can express differential cross section in terms of the electron scattering angle θ or Q^2

$$\frac{d\sigma}{dQ^2} = \frac{4\pi\alpha^2}{Q^4} \left[\frac{G_E^2 + \tau G_M^2}{(1+\tau)} \left(1 - y - \frac{M^2 y^2}{Q^2} \right) + \frac{1}{2} y^2 G_M^2 \right]$$

Inelastic Scattering: We have two independent variables. Therefore need a double differential cross section

$$\frac{d\sigma}{dx dQ^2} = \frac{2\pi\alpha^2}{xQ^4} (Y_+ F_2(x, Q^2) \pm Y_- x F_3(x, Q^2) - y^2 F_L(x, Q^2))$$

Note: The **form factors** have been replaced by the **structure functions**. They can not be interpreted as the Fourier transforms of the charge and magnetic moment distributions. They describe the momentum distribution of the quarks within the proton.

Parton Distribution Functions (PDFs)

The **factorization theorem** states that the structure functions F_i can be written as the convolution of the nonperturbative parts and the hard coefficient functions which can be calculated in pQCD.

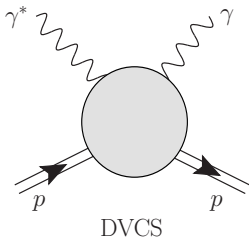
$$F_i(x, Q^2) = \sum_{a=q,g} C_{i,a}(\alpha_s, Q^2) \otimes f_a(x, Q^2)$$

$xf_a(x, Q^2) \equiv$ **Parton Distribution Functions (PDFs)**

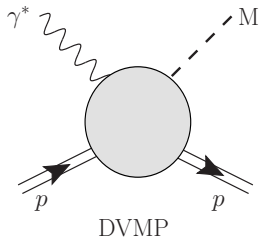
Question: What about Form Factors???

Generalized Parton Distributions (GPDs)

Experiment

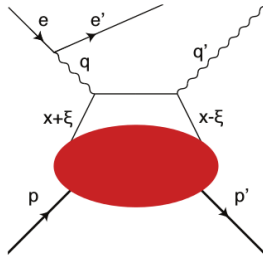


Deeply Virtual Compton Scattering



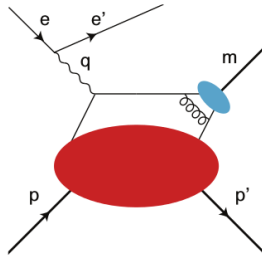
Deeply Virtual Meson Production

Factorization Theorem



(a) Deeply virtual Compton scattering.

$$t = (p' - p)^2$$



(b) Deeply virtual meson production.

$$\xi \equiv \text{skewness}$$

GPDs

- Generalized parton distributions (GPDs), are universal non-perturbative objects entering the description of hard exclusive electroproduction processes.
- GPDs depend on more variables (x, ξ, t, Q^2) .
- GPDs display the characteristic properties to present a three-dimensional (3D) description of hadrons.
- GPDs are a generalization of PDFs and FFs.
- PDFs can be recovered from GPDs (in the so-called forward limit) by setting to zero the extra variables in GPDs.

GPDs VS Observables

Electromagnetic FFs

$$\frac{d\sigma}{dQ^2} = \frac{4\pi\alpha^2}{Q^4} \left[\frac{G_E^2 + \tau G_M^2}{(1 + \tau)} \left(1 - y - \frac{M^2 y^2}{Q^2} \right) + \frac{1}{2} y^2 G_M^2 \right]$$

The Dirac and Pauli form factors, F_1^i and F_2^i , are related to the Sachs form factors by

$$G_M^i = F_1^i + F_2^i, \quad G_E^i = F_1^i + \frac{t}{4m^2} F_2^i, \quad (3)$$

where m is the nucleon mass and again $i = p, n$. One can further decompose

$$\begin{aligned} F_i^p &= e_u F_i^u + e_d F_i^d + e_s F_i^s, \\ F_i^n &= e_u F_i^d + e_d F_i^u + e_s F_i^s, \end{aligned} \quad (4)$$

Electromagnetic FFs

The flavor form factors can be written in terms of GPDs at zero skewness. For each quark flavor we have the sum rules

$$F_1^q(t) = \int_0^1 dx H_v^q(x, t), \quad F_2^q(t) = \int_0^1 dx E_v^q(x, t) \quad (7)$$

with

$$\begin{aligned} H_v^q(x, t) &= H^q(x, 0, t) + H^q(-x, 0, t), \\ E_v^q(x, t) &= E^q(x, 0, t) + E^q(-x, 0, t), \end{aligned} \quad (8)$$

$$H^q(x, 0, 0) = q(x) \quad \text{and} \quad H^q(-x, 0, 0) = -\bar{q}(x)$$

Axial FFs and Nucleon Radii

$$G_A(t) = \int_0^1 dx [\tilde{H}_v^u(x, t) - \tilde{H}_v^d(x, t)] \\ + 2 \int_0^1 dx [\tilde{H}^{\bar{u}}(x, t) - \tilde{H}^{\bar{d}}(x, t)].$$

$$\langle r_{jE}^2 \rangle = 6 \frac{dG_E^j}{dt} \Big|_{t=0},$$

$$\langle r_{jM}^2 \rangle = \frac{6}{\mu_j} \frac{dG_M^j}{dt} \Big|_{t=0},$$

Wide-angle Compton scattering (WACS)

$$\frac{d\sigma}{dt} = \frac{\pi\alpha_{\text{em}}^2}{s^2} \frac{(s-u)^2}{-us} \left[R_V^2(t) - \frac{t}{4m^2} R_T^2(t) + \frac{t^2}{(s-u)^2} R_A^2(t) \right].$$

$$R_V = \sum_q e_q^2 \int_0^1 \frac{dx}{x} [H_v^q(x, t) + 2H^{\bar{q}}(x, t)],$$

$$R_T = \sum_q e_q^2 \int_0^1 \frac{dx}{x} [E_v^q(x, t) + 2E^{\bar{q}}(x, t)],$$

$$R_A = \sum_q e_q^2 \int_0^1 \frac{dx}{x} [\tilde{H}_v^q(x, t) + 2\tilde{H}^{\bar{q}}(x, t)].$$

Determination of GPDs

Model for GPDs

The valence GPDs H_V^q , for example, can be related to ordinary valence PDFs as

$$H_V^q(x, t, \mu^2) = q_V(x, \mu^2) \exp[tf_q(x)].$$

The profile functions $f_q(x)$ can have the simple form

$$f_q(x) = \alpha'(1-x) \log \frac{1}{x}.$$

Model for GPDs

The behavior of profile function $f(x)$ can be well characterized by the forms

$$f_q(x) = \alpha'(1-x)^2 \log \frac{1}{x} + B_q(1-x)^2 + A_q x(1-x),$$

and

$$f_q(x) = \alpha'(1-x)^3 \log \frac{1}{x} + B_q(1-x)^3 + A_q x(1-x)^2.$$

Global Analysis?

It is well known now that several exclusive processes can provide information on GPDs.

- The elastic electron-proton scattering
- Deeply virtual Compton scattering (DVCS)
- Deeply virtual meson production (DVMP)
- The nucleon axial form factor
- Wide-angle Compton scattering (WACS)
- Heavy vector meson production
- Double deeply virtual Compton scattering
- Exclusive pion- or photon-induced lepton pair production

Project 1

Nucleon axial form factor from generalized parton distributions

Hadi Hashamipour,^{1,*} Muhammad Goharipour,^{2,†} and Siamak S. Gousheh^{1,‡}

¹*Department of Physics, Shahid Beheshti University, General Campus, Evin, Tehran 19839, Iran*

²*School of Particles and Accelerators, Institute for Research in Fundamental Sciences (IPM), PO Box 19568-36681 Tehran, Iran*



(Received 13 March 2019; revised manuscript received 1 June 2019; published 9 July 2019)

It is well established that the nucleon form factors can be related to generalized parton distributions (GPDs) through sum rules. On the other hand, GPDs can be expressed in terms of parton distribution functions (PDFs) according to the Diehl, Feldmann, Jakob, and Kroll (DFJK) model. In this work, we use this model to calculate polarized GPDs for quarks (\tilde{H}_q) using the available polarized PDFs obtained from the experimental data and then study the axial form factor of nucleon. We determine parameters of the model using standard χ^2 analysis of experimental data. It is shown that some parameters should be readjusted, as compared to some previously reported values, to obtain better consistency between the theoretical predictions and experimental data. Moreover, we study in detail the uncertainty of nucleon axial form factor due to various sources.

DOI: [10.1103/PhysRevD.100.016001](https://doi.org/10.1103/PhysRevD.100.016001)

Project 2

Determination of generalized parton distributions through a simultaneous analysis of axial form factor and wide-angle Compton scattering data

Hadi Hashamipour,^{1,*} Muhammad Goharipour,^{2,†} and Siamak S. Gousheh^{1,‡}

¹*Department of Physics, Shahid Beheshti University, G.C., Evin, Tehran 19839, Iran*

²*School of Particles and Accelerators, Institute for Research in Fundamental Sciences (IPM), PO Box 19568-36681, Tehran, Iran*

 (Received 17 June 2020; accepted 20 October 2020; published 12 November 2020)

In this work, we present a new set of unpolarized (H) and polarized (\tilde{H}) generalized parton distributions (GPDs) that have been determined using a simultaneous χ^2 analysis of the nucleon axial form factor (AFF) and wide-angle Compton scattering (WACS) experimental data at the next-to-leading order (NLO) accuracy in QCD. We explore various Ansatzes presented in the literature for GPDs, which use forward parton distributions as input, and choose the ones most suited to our analysis. The experimental data included in our analysis cover a wide range of the squared transverse momentum, which is $0.025 < -t < 6.46 \text{ GeV}^2$. We show that the WACS data affect significantly the large $-t$ behavior of \tilde{H} . The polarized GPDs obtained from the simultaneous analysis of AFF and WACS data differ considerably from the corresponding ones obtained by analyzing AFF and WACS separately, and have less uncertainties. We show that the theoretical predictions obtained using our GPDs are in good agreement with the analyzed AFF and WACS data for the entire range of $-t$ studied. Finally, we obtain the impact parameter dependent parton distributions, both in an unpolarized and in a transversely polarized proton, and present them as tomography plots.

DOI: 10.1103/PhysRevD.102.096014

Project 3

Determination of the generalized parton distributions through the analysis of the world electron scattering data considering two-photon exchange corrections


Hadi Hashamipour,^{1,†} Muhammad Goharipour^{2,1,*}, K. Azizi,^{2,3,1,‡} and S. V. Goloskokov^{4,§}

¹*School of Particles and Accelerators, Institute for Research in Fundamental Sciences (IPM), P.O. Box 19395-5746, Tehran, Iran*

²*Department of Physics, University of Tehran, North Karegar Avenue, 14395-547, Tehran, Iran*

³*Department of Physics, Doğuş University, Acıbadem-Kadıköy, 34722 Istanbul, Turkey*

⁴*Bogoliubov Laboratory of Theoretical Physics, Joint Institute for Nuclear Research, Dubna 141980, Moscow region, Russia*

 (Received 3 November 2021; accepted 18 February 2022; published 4 March 2022)

We determine the valence generalized parton distributions (GPDs) H_1^q and E_1^q with their uncertainties at zero skewness by performing a χ^2 analysis of the world electron scattering data considering two-photon exchange corrections. The data include a wide and updated range of the electric and magnetic form factors (FFs) of the proton and neutron. As a result, we find that there are not enough constraints on GPDs E_1^q from FFs data solely though H_1^q are well constrained. By including the new data of the charge and magnetic radius of the nucleon in the analysis, we show that they put new constraints on the final GPDs, especially on E_1^q . Moreover, we calculate the gravitational FF M_2 and the total angular momentum J^q using the extracted GPDs and compare them with the FFs obtained from the light-cone QCD sum rules (LCSR) and lattice QCD. We show that our results are interestingly in a good consistency with the pure theoretical predictions.

DOI: [10.1103/PhysRevD.105.054002](https://doi.org/10.1103/PhysRevD.105.054002)

New Project

Generalized parton distributions at zero skewness

Hadi Hashamipour^{a,*}, Muhammad Goharipour^{b,a,†}, K. Azizi^{b,c,a,‡} and S.V. Goloskokov^{d§}

^a*School of Particles and Accelerators, Institute for Research in Fundamental Sciences (IPM), P.O. Box 19395-5746, Tehran, Iran*

^b*Department of Physics, University of Tehran, North Karegar Avenue, Tehran 14395-547, Iran*

^c*Department of Physics, Doğuş University, Acıbadem-Kadıköy, 34722 Istanbul, Turkey*

^d*Bogoliubov Laboratory of Theoretical Physics, Joint Institute for Nuclear Research, Dubna 141980, Moscow region, Russia*

(Dated: November 18, 2022)

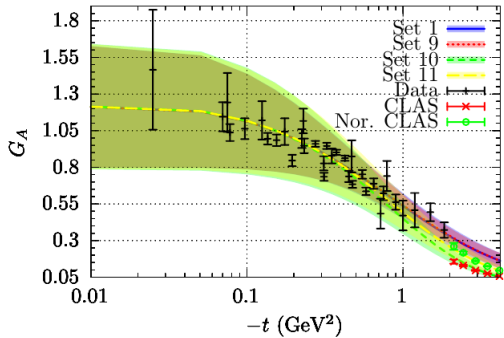
In this study, we present a new determination of the generalized parton distributions (GPDs) with their uncertainties at zero skewness, $\xi=0$, through a simultaneous analysis of all available experimental data of the nucleon electromagnetic form factors (FFs), nucleon charge and magnetic radii, proton axial FF (AFF), and wide-angle Compton scattering (WACS) cross section for the first time. This can be considered as the most comprehensive analysis of GPDs at $\xi=0$ performed so far. We show that such an analysis provides the simultaneous determination of three kinds of GPDs, namely H^q , \tilde{H}^q and E^q , considering also the sea quark contributions. As a result, we find that the inclusion of the WACS and AFF data at larger values of the momentum transfer squared can put new constraints on GPDs and change them drastically in some cases. We also indicate that the results for the gravitational FF M_2 and the proton total angular momentum J^p calculated using the extracted GPDs are in more agreement with the light-cone QCD sum rules (LCSR) and lattice QCD predictions when all experimental data are included in the analysis simultaneously and the sea quark contributions are considered.

Result

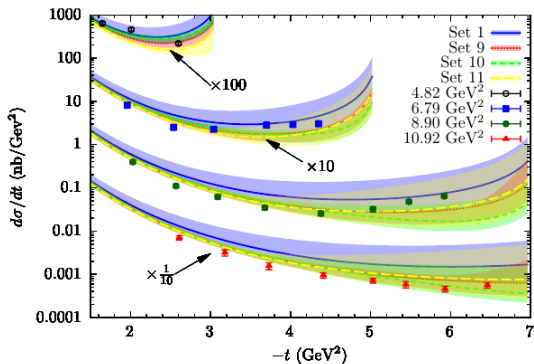
TABLE V. The results of the analyses including the WACS data [74] considering two different scenarios of Eq. (6). See Sec. IV C for more details.

Observable	$-t$ (GeV ²)	$\chi^2/N_{\text{pts.}}$					
		Scenario 2			Scenario 3		
		Set 6	Set 7	Set 8	Set 9	Set 10	Set 11
G_M^p [64]	0.0152 – 0.5524	489.6/77	485.8/77	486.6/77	486.6/77	485.3/77	488.6/77
$G_M^p/\mu_p G_D$ [61]	0.007 – 32.2	108.7/56	108.0/56	107.1/56	110.7/56	107.8/56	109.0/56
$R^p = \mu_p G_E^p/G_M^p$ [62]	0.162 – 8.49	107.3/69	107.6/69	106.1/69	107.5/69	106.8/69	104.9/69
G_E^n [62]	0.00973 – 3.41	49.7/38	52.1/38	44.5/38	52.1/38	51.8/38	45.1/38
$G_M^n/\mu_n G_D$ [62]	0.071 – 10.0	52.6/33	53.6/33	54.3/33	54.5/33	53.3/33	54.0/33
G_A [67–72]	0.025 – 1.84	129.6/34	154.1/34	135.1/34	129.8/34	162.6/34	138.2/34
G_A [73]	2.12 – 4.16	–	62.3/5	3.5/5	–	49.0/5	3.0/5
$\sqrt{\langle r_{pE}^2 \rangle}$ [58]	0	0.0/1	0.1/1	0.2/1	0.0/1	0.0/1	0.0/1
$\sqrt{\langle r_{pM}^2 \rangle}$ [58]	0	1.6/1	1.5/1	1.5/1	1.6/1	1.5/1	1.7/1
$\langle r_{nE}^2 \rangle$ [58]	0	2.9/1	3.2/1	6.1/1	2.6/1	4.1/1	4.3/1
$\sqrt{\langle r_{nM}^2 \rangle}$ [58]	0	20.2/1	23.2/1	22.8/1	17.6/1	23.1/1	22.4/1
$d\sigma/dt$ (WACS) [74]	1.65 – 6.46	431.3/25	453.8/25	503.5/25	284.7/25	371.5/25	330.4/25
Total $\chi^2/\text{d.o.f.}$		1393.5/316	1505.3/321	1471.3/321	1247.7/316	1416.8/321	1301.6/321

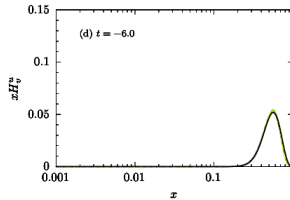
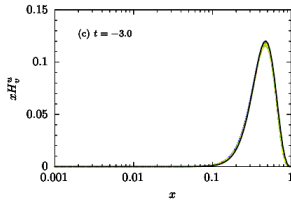
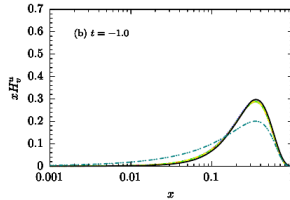
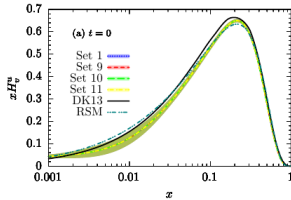
Comparison with data



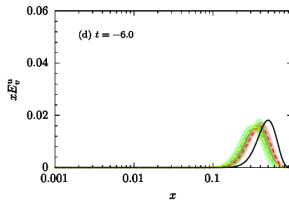
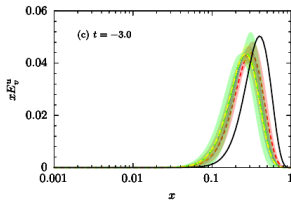
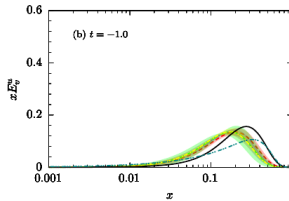
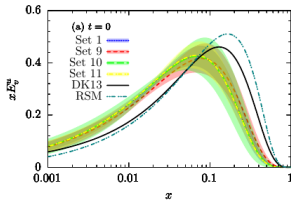
Comparison with data



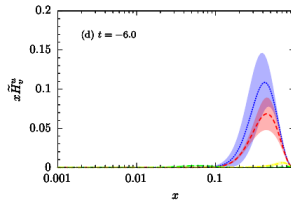
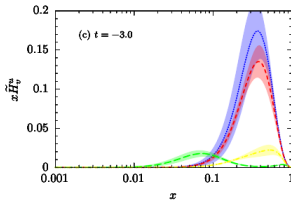
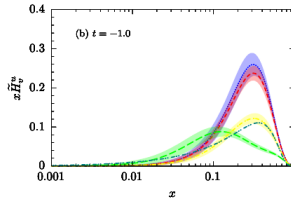
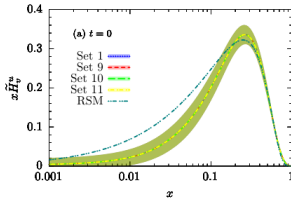
Extracted GPDs



Extracted GPDs



Extracted GPDs

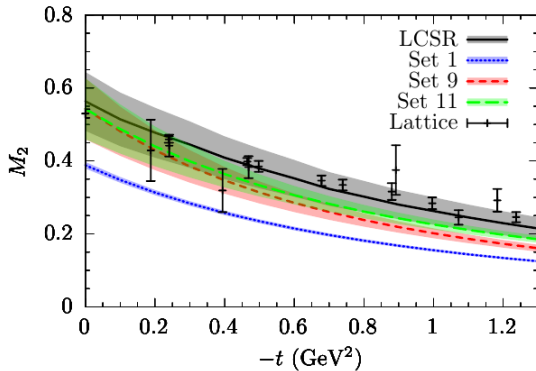


Comparison with other quantities

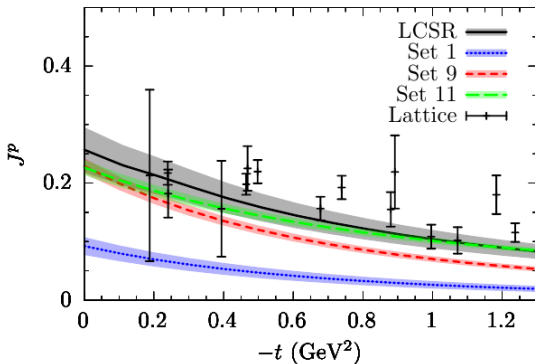
$$\int_{-1}^1 dx x \sum_q H^q(x, \xi, t) = M_2(t) + \frac{4}{5} \xi^2 d_1(t),$$

$$\int_{-1}^1 dx x [H^q(x, t) + E^q(x, t)] = \frac{1}{2} J^q(t).$$

Gravitational Form Factor



Total angular momentum

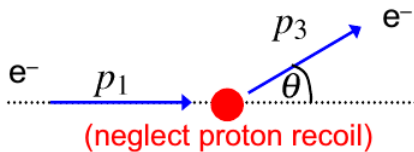


Conclusions

- We performed a new determination of GPDs with their uncertainties at zero skewness, $\xi=0$, through a simultaneous analysis of all available experimental data of the nucleon electromagnetic FFs, nucleon charge and magnetic radii, proton axial FFs, and WACS for the first time. This can be considered as the most comprehensive analysis of GPDs at $\xi=0$ performed so far.
- New precise measurements of various observables are needed to put more constraints on GPDs and answer to present open questions.

Backup

Rutherford Scattering Revisited



Rutherford scattering is the low energy limit where the recoil of the proton can be neglected and the electron is non-relativistic

$$\left(\frac{d\sigma}{d\Omega} \right)_{\text{Rutherford}} = \frac{\alpha^2}{16E_K^2 \sin^4 \theta / 2}$$

The Mott Scattering Cross Section

- For Rutherford scattering we are in the limit where the target recoil is neglected and the scattered particle is non-relativistic $E_K \ll m_e$
- The limit where the target recoil is neglected and the scattered particle is **relativistic** (i.e. just neglect the electron mass) is called Mott Scattering
- It is then straightforward to obtain the result:

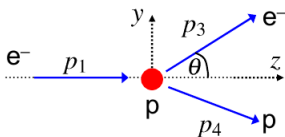
$$\rightarrow \left(\frac{d\sigma}{d\Omega} \right)_{\text{Mott}} = \underbrace{\frac{\alpha^2}{4E^2 \sin^4 \theta/2}}_{\text{Rutherford formula}} \underbrace{\cos^2 \frac{\theta}{2}}_{\text{Overlap between initial/final state electron wave-functions. Just QM of spin } 1/2}$$

Rutherford formula
 with $E_K = E$ ($E \gg m_e$)

**Overlap between initial/final
 state electron wave-functions.
 Just QM of spin $1/2$**

Point-like Electron-Proton Elastic Scattering

- So far have only considered the case we the proton does not recoil...
 For $E_1 \gg m_e$ the general case is



$$p_1 = (E_1, 0, 0, E_1)$$

$$p_2 = (M, 0, 0, 0)$$

$$p_3 = (E_3, 0, E_3 \sin \theta, E_3 \cos \theta)$$

$$p_4 = (E_4, \vec{p}_4)$$

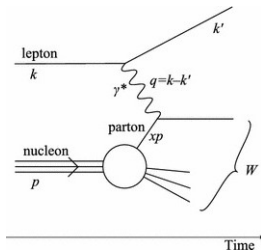
term E_3/E_1 is due to the proton recoil.

$$\frac{d\sigma}{d\Omega} = \frac{\alpha^2}{4E_1^2 \sin^4 \theta/2} \frac{E_3}{E_1} \left(\cos^2 \theta/2 - \underbrace{\frac{q^2}{2M^2} \sin^2 \theta/2}_{\text{magnetic interaction}} \right)$$

- the new term: $\propto \sin^2 \frac{\theta}{2}$ \longleftrightarrow

Magnetic interaction : due to the spin-spin interaction

Deep Inelastic Scattering (DIS)



$$W^2 = (p + q)^2 = M_p^2 + 2p \cdot q + q^2 \quad (1)$$

$W^2 \gg M_p^2 \Rightarrow$ Inelastic scattering

$Q^2 \gg M_p^2 \Rightarrow$ Deep

If $W = M_p$, $Q^2 = -q^2 \Rightarrow x = \frac{Q^2}{2p \cdot q} = 1 \Rightarrow$ elastic scattering

DIS cross section

$$\frac{d\sigma}{dx dy} = x s \frac{d\sigma}{dx dQ^2} = \frac{2\pi y \alpha^2}{Q^4} \sum_j \eta_j L_j^{\mu\nu} W_{\mu\nu}^j \quad (2)$$

$$y = \frac{p \cdot q}{p \cdot k} = \left(\frac{\nu}{E} \right)_{\text{lab.frame}}, \quad s = (k + p)^2 \simeq \frac{Q^2}{xy}$$

DIS cross section

$$\frac{d\sigma}{dx dy} = x s \frac{d\sigma}{dx dQ^2} = \frac{2\pi y \alpha^2}{Q^4} \sum_j \eta_j L_j^{\mu\nu} W_{\mu\nu}^j \quad (2)$$

$$y = \frac{p \cdot q}{p \cdot k} = \left(\frac{\nu}{E}\right)_{\text{lab.frame}}, \quad s = (k + p)^2 \simeq \frac{Q^2}{xy}$$

$$\frac{d\sigma}{dx dQ^2} = \frac{2\pi\alpha^2}{xQ^4} (Y_+ F_2(x, Q^2) \pm Y_- x F_3(x, Q^2) - y^2 F_L(x, Q^2)) \quad (3)$$

$$Y_{\pm} = 1 \pm (1 - y)^2$$

DIS cross section

$$\frac{d\sigma}{dx dy} = xs \frac{d\sigma}{dx dQ^2} = \frac{2\pi y \alpha^2}{Q^4} \sum_j \eta_j L_j^{\mu\nu} W_{\mu\nu}^j \quad (2)$$

$$y = \frac{p \cdot q}{p \cdot k} = \left(\frac{\nu}{E}\right)_{\text{lab.frame}}, \quad s = (k + p)^2 \simeq \frac{Q^2}{xy}$$

$$\frac{d\sigma}{dx dQ^2} = \frac{2\pi\alpha^2}{xQ^4} (Y_+ F_2(x, Q^2) \pm Y_- x F_3(x, Q^2) - y^2 F_L(x, Q^2)) \quad (3)$$

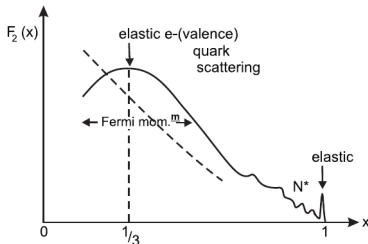
$$Y_{\pm} = 1 \pm (1 - y)^2$$

$$\frac{d^2\sigma}{dx dQ^2} = \frac{2\pi\alpha^2}{xQ^4} [1 + (1 - y)^2] \sum_i e_i^2 x f_i(x), \quad (4)$$

$x f_i(x) \equiv$ **Parton Distribution Functions (PDFs)**

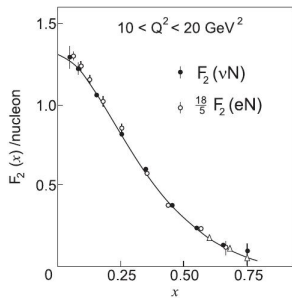
Bjorken scaling violation

Replay : e-proton scattering



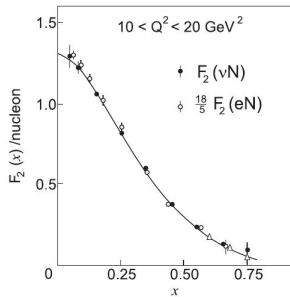
$$F_2(x) = \sum_i e_i^2 x f_i(x), \quad x = \frac{Q^2}{2p \cdot q} \quad \text{Bjorken scaling}$$

Big Puzzle



$$\int_0^1 F_2(\nu N) dx = \int_0^1 \sum_{q, \bar{q}} x f(x) dx \simeq 0.5$$

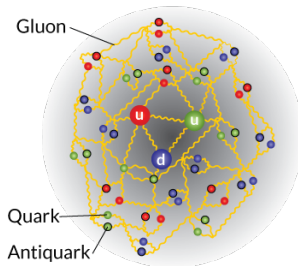
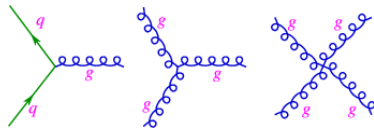
Big Puzzle



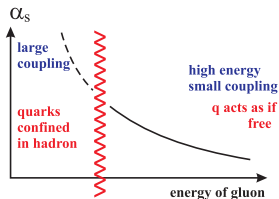
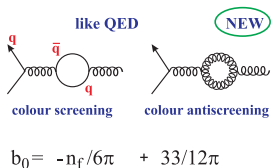
$$\int_0^1 F_2(\nu N) dx = \int_0^1 \sum_{q, \bar{q}} x f(x) dx \simeq 0.5$$

$F_2(x, Q^2) \Leftrightarrow$ Bjorken scaling violation $\Rightarrow f(x, Q^2)$

Quantum chromodynamics (QCD)



Strong coupling constant α_s



For enough large Q^2 , α_s becomes small. So, for a dimensionless QCD observable R we can write,

$$R = \sum_n c_n \alpha_s^n$$

High orders calculations

Calculating high orders terms of the perturbative expansion, two kinds of divergences appear, the ultraviolet and infrared and collinear divergences:

- Ultraviolet divergences (UV), come from the integration over large values of loop momenta, but they are removed after the renormalization of the theory.

$$\alpha_s \Rightarrow \alpha_s(\mu_R^2)$$

- Infrared and collinear divergences appear in the calculation of the Feynman diagrams of the real and virtual corrections in the limit of vanishing energy of an emitted parton or when two partons become collinear. A factorization scale, μ_F , has to be introduced for the removal of these divergences.

$$xf(x) \Rightarrow xf(x, \mu_F^2)$$

QCD Factorization Theorem

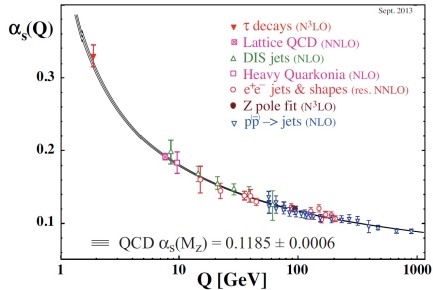
When pQCD can be applied, the factorization theorem states that the cross section of DIS process can be written as the convolution of Parton Distribution Functions (PDFs) and the hard subprocesses.

DIS Cross Section

$$\frac{d\sigma^{ep \rightarrow eX}}{dP} = \sum_f \int dx f(x, \mu_F^2) \times \frac{d\hat{\sigma}^{ef \rightarrow eX'}(\mu_F^2, \alpha_s(\mu_R^2))}{dP}. \quad (5)$$

Since PDFs $xf(x)$ are nonperturbative objects, they cannot be driven from QCD. So, in the standard approach, PDFs are extracted normally by QCD global analyses of the experimental data.

Running α_s



$$\alpha_s(Q^2) = \frac{\alpha_s(\mu^2)}{1 + b_0 \alpha_s(\mu^2) \log(Q^2/\mu^2)} \quad (6)$$

$$b_0 = -\frac{n_f}{6\pi} + \frac{33}{12\pi}$$

DGLAP Evolution Equations

If we have the parton densities as functions of x at an initial scale μ_0^2 , we can obtain them at any arbitrary scale Q^2 by solving the DGLAP equations.

$$\frac{\partial f_i(x, \mu_F^2)}{\partial \ln \mu_F^2} = \sum_{j \in \{q, g\}} \int_x^1 \frac{dz}{z} P_{ij}(z, \alpha_s(\mu_F^2)) f_j(x/z, \mu_F^2), \quad (7)$$

$$P_{ij}(z, \alpha_s(\mu_F^2)) = P_{ij}^{(0)}(z) + \frac{\alpha_s(\mu_F^2)}{2\pi} P_{ij}^{(1)}(z) + \dots \quad (8)$$

$$P_{qq}^{(0)}(x) = \frac{4}{3} \left[\frac{1+x^2}{(1-x)_+} + \frac{3}{2} \delta(1-x) \right]$$

$$P_{gg}^{(0)}(x) = 6 \left[\frac{x}{(1-x)_+} + \frac{1-x}{x} + x(1-x) + \left(\frac{11}{12} - \frac{n_f}{18} \right) \delta(1-x) \right]$$

DGLAP Evolution Equations

Singlet: $q_s = \sum_{i=1}^{n_f} (q_i + \bar{q}_i) \Rightarrow \frac{\partial}{\partial \ln \mu^2} \begin{pmatrix} q_s \\ g \end{pmatrix} = \begin{pmatrix} P_{qq} & P_{qg} \\ P_{gq} & P_{gg} \end{pmatrix} \otimes \begin{pmatrix} q_s \\ g \end{pmatrix}$

non-singlet: $q_{ij}^{\pm} = (q_i \pm \bar{q}_i) - (q_j \pm \bar{q}_j)$ and $q_v = \sum_{i=1}^{n_f} (q_i - \bar{q}_i)$

$$\Rightarrow \frac{\partial q_{ij}^{\pm}}{\partial \ln \mu^2} = P_{\pm} \otimes q_{ij}^{\pm} \quad \text{and} \quad \frac{\partial q_v}{\partial \ln \mu^2} = P_v \otimes q_v,$$

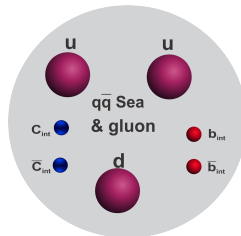
Motivations

- One of the significant aspects of the nucleon structure is the distribution of strange and antistrange sea quarks and their possible asymmetry.
- More precise knowledge in this field is very important for better understanding of the nucleon structure and properties of the sea quarks and also for describing processes such as W boson production in association with charm jets or neutrino interactions.
- **It is proven that the perturbative regime of QCD cannot describe the present experimental evidences for the $s - \bar{s}$ asymmetry.**
- In this way, the nature and dynamical origins of $s - \bar{s}$ asymmetry have always been an interesting subject to research both experimentally and theoretically.

BHPS Model

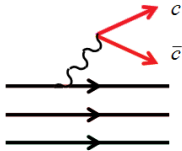
In 1980, Brodsky, Hoyer, Peterson, Sakai (BHPS) suggested the existence of “intrinsic” charm¹ to explain unexpected experimental results:

$$|p\rangle = \mathcal{P}_{3q}|uud\rangle + \underbrace{\mathcal{P}_5^{c\bar{c}}}_{0.01}|uudc\bar{c}\rangle + \dots$$



¹S.J. Brodsky, P. Hoyer, C. Peterson, and N. Sakai, Phys. Lett. B 93, 451 (1980).

Extrinsic VS Intrinsic

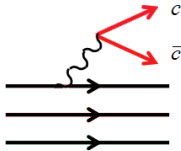


"extrinsic"



"intrinsic"

Extrinsic VS Intrinsic



"extrinsic"

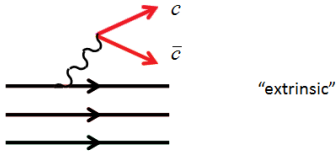


"intrinsic"

Charm pair comes from the QCD DGLAP evolution.

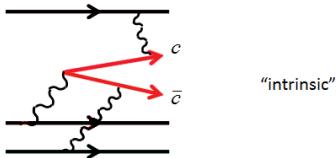
Charm pair was there before evolution.

Extrinsic VS Intrinsic



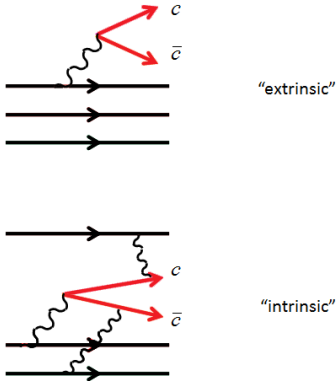
Charm pair comes from the QCD
DGLAP evolution.

Perturbative QCD OK !



Charm pair was there before evolution.
Strong non-perturbative effects.

Extrinsic VS Intrinsic



Charm pair comes from the QCD DGLAP evolution.

Perturbative QCD OK !

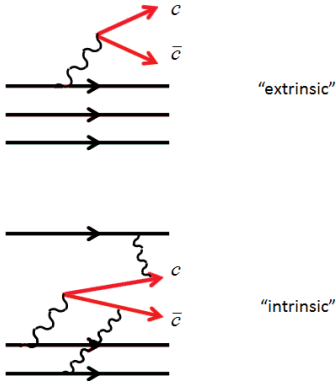
The extrinsic charm has a sea-like characteristics with large magnitude only a the small x region.

Charm pair was there before evolution.

Strong non-perturbative effects.

The intrinsic charm is valencelike with a distribution peaking at larger x .

Extrinsic VS Intrinsic



Charm pair comes from the QCD DGLAP evolution.

Perturbative QCD OK !

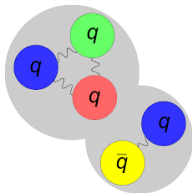
The extrinsic charm has a sea-like characteristics with large magnitude only a the small x region.

Charm pair was there before evolution.

Strong non-perturbative effects.

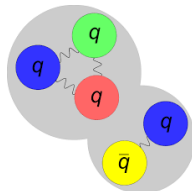
The intrinsic charm is valencelike with a distribution peaking at larger x .

Meson-Baryon Model (MBM)



$$\begin{aligned}
 |N\rangle_{physical} = & \sqrt{Z} |N\rangle_{bare} + \sum_{MB} \sum_{\lambda\lambda'} \int dy d^2\mathbf{k}_\perp \phi_{MB}^{\lambda\lambda'}(y, k_\perp^2) \\
 & \times |M^\lambda(y, \mathbf{k}_\perp); B^{\lambda'}(1-y, -\mathbf{k}_\perp)\rangle.
 \end{aligned} \tag{9}$$

Meson-Baryon Model (MBM)



$$\begin{aligned}
 |N\rangle_{physical} = & \sqrt{Z} |N\rangle_{bare} + \sum_{MB} \sum_{\lambda\lambda'} \int dy d^2\mathbf{k}_\perp \phi_{MB}^{\lambda\lambda'}(y, k_\perp^2) \\
 & \times |M^\lambda(y, \mathbf{k}_\perp); B^{\lambda'}(1-y, -\mathbf{k}_\perp)\rangle.
 \end{aligned} \tag{9}$$

The main virtue of the meson-baryon model compared with the BHPS model is that it can lead to the $q - \bar{q}$ asymmetry in the nucleon sea.

$s - \bar{s}$ asymmetry

$$s^N(x) = \sum_{BM} \int_x^1 \frac{d\bar{y}}{\bar{y}} f_{BM}(\bar{y}) s_B\left(\frac{x}{\bar{y}}\right)$$
$$\bar{s}^N(x) = \sum_{MB} \int_x^1 \frac{dy}{y} f_{MB}(y) \bar{s}_M\left(\frac{x}{y}\right)$$

There are two origins cause this asymmetry:

- First is the difference between the probability distributions of the meson and baryon in the proton
- Second is the difference between the strange and antistrange distributions in the baryon and meson, respectively

$s - \bar{s}$ asymmetry

For the case of intrinsic strange, we can consider six fluctuations as follows:

$$\begin{aligned}
 p &\longrightarrow K^+(u\bar{s})\Lambda^0(uds), \\
 p &\longrightarrow K^0(d\bar{s})\Sigma^+(uus), \\
 p &\longrightarrow K^+(u\bar{s})\Sigma^0(uds), \\
 p &\longrightarrow K^{*+}(u\bar{s})\Lambda^0(uds), \\
 p &\longrightarrow K^{*0}(d\bar{s})\Sigma^+(uus), \\
 p &\longrightarrow K^{*+}(u\bar{s})\Sigma^0(uds).
 \end{aligned}$$

Due to high equality of the K^0 and K^+ , K^{*0} and K^{*+} , and also Λ and Σ physical masses, only two states $K^+\Lambda^0$ and $K^{*+}\Lambda^0$ lead to the different shapes for s and \bar{s} distributions in the nucleon and thus the $s - \bar{s}$ asymmetry.

